



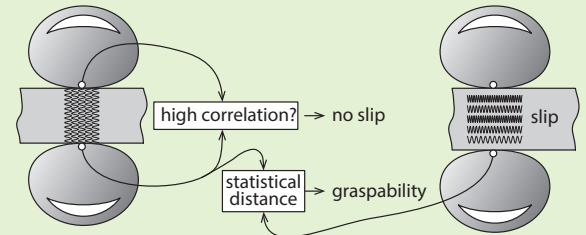
## Robust detection of absence of slip in robot hands and feet

Yerkebulan Massalim , Zhanat Kappassov *Member, IEEE* ,

Huseyin Atakan Varol *Senior Member, IEEE*  and Vincent Hayward *Fellow, IEEE* 

**Abstract**—We describe an algorithm that can robustly decide whether a grip or a footstep is secure given data collected from at least two independent sensors. This algorithm is based on the observation that if there is an absence of slip, then, owing to the high velocity of mechanical waves in solids, the two sensor signals must be highly correlated, even in the presence of internal or external perturbations. The statistical distance between signals collected during slip and non-slip phases, regarded as random distributions, also provides a continuous measure of graspability or walkability of an object being held or a ground being stepped on. We tested the algorithm on a bench using micro-electro-mechanical system (MEMS) accelerometers and with a variety of materials of different surface roughnesses. We also discuss the applications of this non-slip/slip discrimination algorithm and its putative relationship with human gripping behavior.

**Index Terms**—Slip detection, tactile sensing, haptic manipulation, dexterous manipulation.



### I. INTRODUCTION

Manipulation and locomotion crucially depend on friction. When the tangential load sustained by two surfaces in contact exceeds a threshold, slip takes place. Owing to numerous factors, the frictional properties of contacts are difficult to predict. However, successful manipulation and locomotion depend on the absence of slip between the appendages of a robot and external objects. In robotics, sensing techniques able to detect slip have long been recognized to be essential for dexterous manipulation and secure locomotion.

One approach to slip detection is an attempt to imitate the features of the glabrous skin of primates. As early as the 1970s, there were efforts to create sensitive artificial skins for grip adjustment [1]. These approaches are discussed in numerous surveys [2]–[5]. Nevertheless, the neural processes that subserve slip detection during grip adjustment are still not fully explained [6], [7]. Another approach is to take advantage of mechanical load sensors that can be integrated into robot extremities, leading to another family of approaches termed

*intrinsic sensing* [8]. Intrinsic sensing can also be applied to slip detection [9].

Sensors or systems of sensors do not detect slip *per se*. Sensors report some aspects of the consequences of slip in order to trigger appropriate corrective actions. Examples of such actions include tightening a grip, reconfiguring fingers, reducing stride impetus, or adapting posture. Slip detection is accomplished by algorithms that use sensor data to decide that slip has occurred, or is about to occur, between an extremity and an external object. Numerous algorithms surveyed in the next section are tailored to the type of sensor used to collect mechanical signals.

The present article describes an algorithm that depends only weakly on the type of sensor used to collect mechanical signals. An essential requirement for its operation, however, is that there must be at least two sensors signals reporting mechanical events arising from contacts with a single common object. The algorithm could be extended to multiple sensors but two are sufficient.

Slip between surfaces is always associated with a noisy component corresponding to velocity fluctuations caused by brief occurrences of negative damping in frictional phenomena. Sliding surfaces, hard or soft, rough or smooth, even lubricated, all produce frictional noise. The magnitude and the properties of frictional noise depend on a number of factors. These include the materials in contact, the net sliding velocity, the topography of the surfaces, the internal structure of the object, the load, abrasion, interstitial contaminants, and the history of the contact [10]–[12].

Frictional fluctuations can have periodicity, as in squeals or bow-string interactions, but are often predominantly stochastic. Fluctuations are observed even when friction is extremely

Submitted August 2021 and revised month year.

Corresponding author: Z. Kappassov.

Y. Massalim was with the Robotics Department, Nazarbayev University, Nur-Sultan, Kazakhstan and is now with Actronika SAS, 157 boulevard MacDonald, 75019 Paris, France (e-mail: yerkebulan.massalim@actronika.com).

Z. Kappassov and H. A. Varol are with the Robotics Department, Nazarbayev University, Nur-Sultan, Kazakhstan (e-mail: {zhkappassov, ahvarol}@nu.edu.kz).

V. Hayward is with Sorbonne Université, Institut des Systèmes Intelligents et de Robotique (ISIR), 5 place Jussieu, 75005, Paris, France and Actronika SAS, 157 boulevard MacDonald, 75019 Paris, France (e-mail: vincent.hayward@sorbonne-universite.fr).

This work was supported by MES of Kazakhstan, Grant number AP09058050.

low [13]. Slip detection should be robust to many possible perturbations, for example, vibrations arising from the robot's actuators and transmissions or from the interactions of a gripped object with external objects.

Slip detection ought to be free from as many assumptions as possible, i.e., independent of the assumed models of friction. To progress toward this goal, we propose that an *absence of slip* can be reliably determined during a grip or a footstep, by investigating the similarity between signals from sensors responding to contact with a common solid object. In the absence of slip, the signals exhibit a high degree of similarity since the wavelength of mechanical waves in solids is generally much greater than the distance between two sensors. At one thousand Hertz, the wavelength of mechanical waves in wood is about five meters; in granular materials, such as soils, it is of the order of fifty centimeters [14], [15].

## II. RELATED WORKS

In order to achieve robotic manipulation, the detection of slip was viewed as an imperative necessity early on. Hirochika Inoue [16] concluded, "Force feedback enables the robot to guide a peg into a hole quite reliably given that the parts do not slip in the hand. From a practical point of view, it is also important to develop a general-purpose hand that prevents 'slip' or that at least detects its occurrence".

Baits et al. [17] had already demonstrated automatic grip adjustment by detecting vibrations using piezoelectric sensors in contact with a gripped object. At the same time, Ring and Welburn [18] observed the Cattaneo-Mindlin contact mechanics in human fingers acting against a rigid counter surface. The Cattaneo-Mindlin contact mechanics describes partially sliding contacts as a mixture of stick and sliding regions. They noted the time course for the transition to fully-developed slip to last about 300 ms (value later confirmed in [19]) and developed a sensor designed to directly resolve the state of a contact.

Research in hand prostheses anticipated the need to detect slip, ushering families of methods concerned with the analysis of the temporal properties of sensor signals available in a gripping device (Section II-A); the analysis of the spatio-temporal evolution of a population of sensors (Section II-B); and the resolution of contact states from force measurements (Section II-C). Efforts have been made to develop sensing techniques to measure slip directly (Section II-D). Although the literature on slip detection is often intertwined with the description of tactile sensors, the above classification can guide the discussion of slip detection algorithms.

### A. Temporal Properties of Tactile Signals

Dornfeld and Handy [20] pointed out the possibility of taking advantage of the acoustic emissions of sliding contacts to detect slip. Howe and Cutkosky [21] proposed to threshold the amplitude of the signal given by a miniature accelerometer integrated in a flexible envelope wrapped around a robot finger. Tremblay and Cutkosky [22] observed that the slip signal was more reliably detected from accelerometers located away from the region of contact. Kyberd and Chappell [23] described an algorithm that computed a discrete approximation of the

temporal gradient of signals arising from force-sensing resistors in the palm and fingertips of a multi-fingered prosthetic hand. This algorithm gave an approximation of the direction of object slip. Later, Kyberd et al. [24] discussed the automatic tightening of a grip from cumulative counts of slip events detected by microphones in the fingers of a prosthetic hand. Goger et al. [25] employed the short-term Fourier transform to process a signal given by a piezoelectric polyvinylidene difluoride (PVDF) polymer sensor. The frequency-domain representation was further processed through feature detection and nearest-neighbor classification to decide whether a slip occurred. Takenawa [26] embedded miniature magnets in artificial skin. By Lenz's law, the oscillation of these magnets induced voltages in neighboring coils. The occurrence of slip was decided through the detection of spikes caused by the release of stored elastic energy. In another work, researchers placed accelerometers in the grippers of a robot [27]. During grip, the slip was detected from the magnitude of the signal during specific phases of the manipulation. Taking advantage of a piezoresistive film sensor, Teshigawara et al. [28] used the Haar discrete wavelet transform (DWT) to detect specific signal fluctuations that were indicative of slip. Heyneman and Cutkosky [29] observed that under the assumption of linearity the mapping from input vibrations to the sensor outputs is the sum of the signal resulting from the coupling object-finger and the vibrations of the held object. The analysis of coherence among sensor signals in the frequency domain enabled the offline classification of slip types from data recorded by a robot gripper with two BioTac sensors (Syntouch, Montrose, CA). Using a single BioTac sensor, Su et al. [30] used an artificial neural network comprising a fifty-neuron hidden layer to classify slips into sliding and pivoting contacts. Veiga et al. [31], also with BioTac sensors, programmed a support vector machine to predict slip using features extracted from raw sensor data.

### B. Spatio-Temporal Evolution of a Population of Sensors

Stojiljković and Clot [1] covered a prosthetic hand with a soft artificial skin made of an electrically conductive elastomer. The inner layer of this skin featured a dense array of electrodes. Contact with objects reduced the resistance of each cell. Each sensing cell produced one slowly-adapting output and one fast-adapting output. An artificial neural network implemented a *lateral inhibition* algorithm that provided separate fast-adapting excitatory and slowly-adapting inhibitory signals. These signals were combined to detect spatial and temporal mechanical gradients whose magnitude determined the activation of the motors. This way, the slip was prevented for both soft and hard gripped objects. From prior work suggesting the use of stochastic filtering to process data available from a population of sensors [32], Ho and Hirai [33] used image processing to estimate the ratio of the stuck contact area to the gross contact area to adjust grip during bi-digital object lifting. Yuan et al. [34] collected dense data using a GelSight sensor [35] and used image processing to estimate the state of the Cattaneo-Mindlin contact mechanics. Meier et al. [36] used data acquired from arrays of piezoresistive sensors pressed

against a rigid object and, from features extracted in the frequency domain, trained a convolutional neural network to distinguish between sliding and pivoting contacts. Roberge *et al.* [37] used unstructured data acquired from capacitive sensing arrays and converted them to the frequency domain to give a sparse representation of these data. After training, a support vector machine algorithm was able to reliably identify slips within the dataset. James *et al.* [38] used an optical tactile sensor, the TacTip, to collect image-like data during a variety of interactions with surfaces. A support vector machine could accurately detect slip from the temporal evolution of the image data. Rigi *et al.* [39] utilized a neuromorphic event-based vision sensor to identify regions of partial slip from internal generated vibrations during contact between rigid objects.

### C. Contact State Resolution from Force Measurements

Ring and Welburn [18] described a sensor that measures the magnitude of the interaction force between a finger and an object. Thus, assuming a known coefficient of friction, the slip was prevented by driving a single-motor of the two-fingered prosthetic hand proportionally to this signal. The algorithm was similar in its principle to what is realized by an industrial scissor grab lifting clamp with the difference that the gripping action was independent of the direction of external disturbances. Building on the work of Bicchi *et al.* [8] on intrinsic sensing, Melchiorri [40] described a geometrical method to determine the occurrence of slip from the location of the center of rotation of a body in contact with a rigid surface using a combination of force and distributed pressure sensing. Wettels *et al.* [41] used BioTac sensors mounted on an Otto Bock Michelangelo anthropomorphic robotic hand to resolve the contact force through a Kalman filter. Song *et al.* [42] mounted six-axis force/torque sensors on the fingertips of a three-fingered BarrettHand robotic hand and used an extended Kalman filter to estimate the ‘breakaway’ force ratio from the coefficients of a solid friction model, namely the LuGre model [43]. Yussof *et al.* [44] designed a robotic fingertip with forty-one ‘feelers’ whose deflections and compressions were optically measured. The data were used to detect the direction of slip to maintain a stable grip.

### D. Direct Measurement of Slips

Some “computation-free” techniques for slip detection are mentioned in this subsection. Tomović and Stojiljković [45] suggested that because slip is by definition the relative displacement of two surfaces in contact, sensors could be devised to detect slip directly. Notably, one of their designs involved a needle-like pointer set inside an artificial skin layer such that slip entrained its lateral movements, generating trains of electrical pulses by closing a circuit. D’Alessio and Steindler [46] employed contactless inductive transducers. The counter surface, however, was required to possess special magnetic properties. Eghtedari *et al.* [47] took advantage of the properties of a photoelastic layer interposed between a polarizer and an analyzer to produce slip-sensitive fringe patterns that could be imaged. Later, [48] used this principle to produce

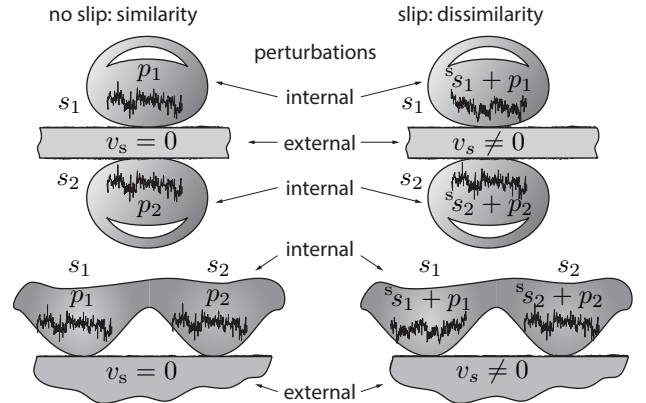


Fig. 1: Under most conditions, in the absence of slip, the signals arising from different sensors must be correlated.

a continuous signal during slip. Gofuku *et al.* [49] installed one illuminator and two adjacent reflected light detectors in a robot gripper. Researchers estimated the slip velocity using signal shift estimation by cross-correlating the two signals in the frequency domain. Accoto *et al.* [50] described a micro-sensor that exploited the dependency of heat diffusion upon the relative velocity of two surfaces in contact to detect slip. Kondratenko *et al.* [51] revisited the technique of the oscillating pin interacting with a held object and sensed the slip-induced oscillations by capacitive detectors.

## III. ALGORITHM FOR ABSENCE OF SLIP DETECTION

The slip conditions for a gripping or a stepping system as in Fig. 1 may be represented by

$$\begin{aligned} \text{no slip: } & \begin{cases} s_1(t) = p_1(t), \\ s_2(t) = p_2(t), \end{cases} & (1) \\ \text{slip: } & \begin{cases} s_1(t) = {}^s s_1(t) + p_1(t), \\ s_2(t) = {}^s s_2(t) + p_2(t). \end{cases} & (2) \end{aligned}$$

where  $s_1(t)$  and  $s_2(t)$  stand for the signals acquired by the sensors,  ${}^s s_1(t)$  and  ${}^s s_2(t)$  the signals arising from frictional noise, and  $p_1(t)$  and  $p_2(t)$  are the signals resulting from unknown external and internal perturbations. As discussed earlier,  $p_1(t)$  and  $p_2(t)$  are expected to be similar since they arise from common sources while  ${}^s s_1(t)$  and  ${}^s s_2(t)$  are expected to be different since they arise from sliding noise.

Cross-correlation is a measure of the similarity between signals. The cross-correlation of two continuous-time signals is computed from their reversed convolution. Since in practice signals are available in discrete time, cross-correlation can be computed over a finite-length window from the inner product of two vectors. In signal analysis, an approach commonly adopted to arrive at a practical algorithm is to consider the signals to be zero-mean random time-series of size  $n$ . We make this assumption for the sensor signals  $s_1(t)$  and  $s_2(t)$ .

The computation of the zero-delay normalized cross-correlation,  $\text{NCC}(s_1, s_2)$  between the two vectors,  $\mathbf{s}_1 = [s_1(0), \dots, s_1(n-1)]^T$  and  $\mathbf{s}_2 = [s_2(0), \dots, s_2(n-1)]^T$  can

then be written as

$$\text{NCC}(\mathbf{s}_1, \mathbf{s}_2) = \frac{\sum_{i=0}^{n-1} s_1(i)s_2(i)}{\sqrt{\sum_{i=0}^{n-1} s_1^2(i) \sum_{i=0}^{n-1} s_2^2(i)}} \quad (3)$$

$$= \frac{\mathbf{s}_1 \cdot \mathbf{s}_2}{n\sqrt{\sigma(\mathbf{s}_1)\sigma(\mathbf{s}_2)}}, \quad (4)$$

where  $\sigma(\mathbf{s}_1)$  and  $\sigma(\mathbf{s}_2)$  represent the variances of  $\mathbf{s}_1$  and  $\mathbf{s}_2$ , respectively and  $\mathbf{s}_1 \cdot \mathbf{s}_2$  denotes the dot product of the vectors  $\mathbf{s}_1$  and  $\mathbf{s}_2$ .

NCC for the non-slip case can be written using (1) and (4) as

$$\text{NCC}(\mathbf{s}_1, \mathbf{s}_2) = \text{NCC}(\mathbf{p}_1, \mathbf{p}_2) = \frac{\mathbf{p}_1 \cdot \mathbf{p}_2}{n\sqrt{\sigma(\mathbf{p}_1)\sigma(\mathbf{p}_2)}}. \quad (5)$$

Since  $\mathbf{p}_1$  and  $\mathbf{p}_2$  are highly correlated, we can write

$$\text{NCC}(\mathbf{p}_1, \mathbf{p}_2) = \frac{\mathbf{p}_1 \cdot \mathbf{p}_2}{n\sqrt{\sigma(\mathbf{p}_1)\sigma(\mathbf{p}_2)}} \approx 1. \quad (6)$$

In other words, NCC for the non-slip case must be close to one. Similarly, in the case of slip, using (2) and (4), NCC can be written,

$$\begin{aligned} \text{NCC}(\mathbf{s}_1, \mathbf{s}_2) &= \frac{(\mathbf{p}_1 + {}^s\mathbf{s}_1) \cdot (\mathbf{p}_2 + {}^s\mathbf{s}_2)}{n\sqrt{\sigma({}^s\mathbf{s}_1 + \mathbf{p}_1)\sigma({}^s\mathbf{s}_2 + \mathbf{p}_2)}} \\ &= \frac{\mathbf{p}_1 \cdot \mathbf{p}_2 + {}^s\mathbf{s}_1 \cdot \mathbf{p}_2 + {}^s\mathbf{s}_2 \cdot \mathbf{p}_1 + {}^s\mathbf{s}_1 \cdot {}^s\mathbf{s}_2}{n\sqrt{\sigma({}^s\mathbf{s}_1 + \mathbf{p}_1)\sigma({}^s\mathbf{s}_2 + \mathbf{p}_2)}}. \end{aligned} \quad (7)$$

Noting that frictional noise signals are uncorrelated with the perturbation signals and with each other, we can assume that,

$${}^s\mathbf{s}_i \cdot \mathbf{p}_j \approx 0 \quad \forall i, j \in \{1, 2\}, \quad (8)$$

$${}^s\mathbf{s}_1 \cdot {}^s\mathbf{s}_2 \approx 0. \quad (9)$$

Substituting (8) and (9) into (7) gives

$$\text{NCC}(\mathbf{s}_1, \mathbf{s}_2) = \frac{\mathbf{p}_1 \cdot \mathbf{p}_2}{n\sqrt{(\sigma({}^s\mathbf{s}_1) + \sigma(\mathbf{p}_1))(\sigma({}^s\mathbf{s}_2) + \sigma(\mathbf{p}_2))}}, \quad (10)$$

and by posing  $k_1 = \sigma({}^s\mathbf{s}_1)/\sigma(\mathbf{p}_1)$  and  $k_2 = \sigma({}^s\mathbf{s}_2)/\sigma(\mathbf{p}_2)$ , (10) becomes

$$\text{NCC}(\mathbf{s}_1, \mathbf{s}_2) = \frac{\mathbf{p}_1 \cdot \mathbf{p}_2}{n\sqrt{\sigma(\mathbf{p}_1)\sigma(\mathbf{p}_2)}} \frac{1}{\sqrt{(1+k_1)(1+k_2)}}. \quad (11)$$

Noting the high correlation of  $\mathbf{p}_1$  and  $\mathbf{p}_2$ , as in (6), we can simplify this expression to

$$\text{NCC}(\mathbf{s}_1, \mathbf{s}_2) \approx \frac{1}{\sqrt{(1+k_1)(1+k_2)}}. \quad (12)$$

We conclude that, counterintuitively, with this algorithm the greater the perturbations are, the more reliable is the detection of an absence of slip. For example, a robot gripping a part may purposefully cause collisions with external objects to reduce the uncertainty of a secure grip. Likewise, a robot may apply an anticipatory, exaggerated load on a foot to ascertain that it would not slip.

An absence of slip can be detected when the NCC measure is close to one and additional information may be obtained from the analysis of the signals. Of particular interest is the possibility of gauging the ‘‘graspability’’ of an object or the ‘‘walkability’’ of a terrain. To this end, a robot may quantify

how frictional noise differs from background perturbation. For example, a smooth slippery surface would be such that the sensor signals are similar whether or not there is slip.

In keeping with a statistical approach, such evaluation may be accomplished through a distance measure between distributions represented by a vector normalized to a vector of the NCC values during slip,  $\bar{\mathbf{s}}$ , and to another vector of NCC values,  $\bar{\mathbf{p}}$ , when there is no slip. A direct measure can be then provided by the Hellinger distance between discrete distributions known for its efficiency and robustness [52]. This distance,  $H(\bar{\mathbf{s}}, \bar{\mathbf{p}})$  can be computed as follows,

$$H^2(\bar{\mathbf{s}}, \bar{\mathbf{p}}) = \frac{1}{2} \sum_{i=0}^{n-1} \left( \sqrt{\bar{s}(i)} - \sqrt{\bar{p}(i)} \right)^2, \quad (13)$$

$$= \frac{1}{2} \left\| \sqrt{\bar{\mathbf{s}}} - \sqrt{\bar{\mathbf{p}}} \right\|_2^2, \quad (14)$$

$$= 1 - \sum_{i=0}^{n-1} \sqrt{\bar{s}(i)\bar{p}(i)}. \quad (15)$$

The Hellinger Distance provides us with a similarity measure of two probability distribution functions. When its absolute value approaches to one, the distribution are totally different. When its value is close to zero, the distributions are similar. This expression allows one to estimate objectively how well the NCC value can discriminate slip from non-slip for in given conditions, giving robustness.

The algorithm could be instantiated with many other similarity measures other than NCC, although this latter measure has the advantage of being particularly economical to compute. For instance, adopting a deterministic approach, the Fréchet distance between  $\mathbf{s}_1$  and  $\mathbf{s}_2$  could be employed to evaluate their similarity. This method could also have a statistical interpretation [53]. Another statistical method could appeal to the Kolmogorov-Smirnov empirical test to compute the probability that the samples in vectors  $\mathbf{s}_1$  and  $\mathbf{s}_2$  or in  $\mathbf{u}$  and  $\mathbf{v}$  were drawn from a common, yet unknown, distribution. Any of these methods is expected to produce qualitatively similar results. The choice of measures, being entirely application-dependent, is not discussed further.

## IV. EXPERIMENTS

### A. Experimental Setup

An experimental setup (see Fig. 2A) was constructed to systematically test the detection algorithm over a wide range of sliding velocities, materials, and interaction forces. This testbed comprised a slider-crank mechanism that moved interchangeable samples against a pair of sensorized robot gripper pads (Model ENG 100, SCHUNK GmbH, Germany) under the action of a speed-reduced DC motor (Model EC 380619, Maxon Group, Switzerland). The samples were guided by four rollers. A slider-crank mechanism with two adjustable hard-stops entrained the movements of the sample while providing periods of rest. The sample came to a stop each time the mechanism came close to a singular configuration. A linear encoder (AEDR-8300, Broadcom, CA, USA) with a resolution of 0.12 mm provided the ‘‘ground truth’’ for the speed of the



sample by the differentiating the encoder signal numerically and smoothing it through a 500-sample moving average.

The gripper pads could be configured to either grip the sample or press against it from the same side, see Figs. 2B and 2C. These components were held in place by a quick-connect aluminum frame defining a coordinate system with the  $x$ -axis along the direction of the movements of the sample and the  $z$ -axis in the plane of the frame, see Fig. 2A.

The sensors were 3-axis MEMS accelerometers (ADXL 335, Analog Devices, MA, USA) rigidly connected to the gripper pads and set against elastomer supports to prevent rattling as shown in Fig. 2D. The  $z$ -axes of the accelerometers were aligned with the  $z$ -axis of the frame. The pads could be oriented around the common  $z$ -axis by an angle  $\alpha$  between the  $x$ -axes of the accelerometers and the frame. Data were acquired by a custom-made analog-to-digital converter board sampling the analog signals at a rate of 8.0 kHz.

### B. Testing Conditions

Testing was performed at three motor speeds (average speeds of the samples: 0.8, 0.16, and 0.24 m/s) and with three materials (aluminum, plastic, and wood). The grasping or pressing forces were set at two levels for each material (see Table I). The gripping configuration was tested at four different angles  $\alpha$  of orientation ( $0^\circ$ ,  $15^\circ$ ,  $30^\circ$ , and  $45^\circ$ ). In the pressing configuration,  $\alpha$  was zero. These parameters resulted in seventy-two ( $3 \times 3 \times 2 \times 4$ ) distinct conditions in the gripping configuration and eighteen ( $3 \times 3 \times 2$ ) conditions in the pressing configuration. Additional external perturbations were caused by placing a vacuum pump producing 110 Hz vibrations in the vicinity of the testbed. Separate tests were performed with glass samples (see the last row of the Table I).

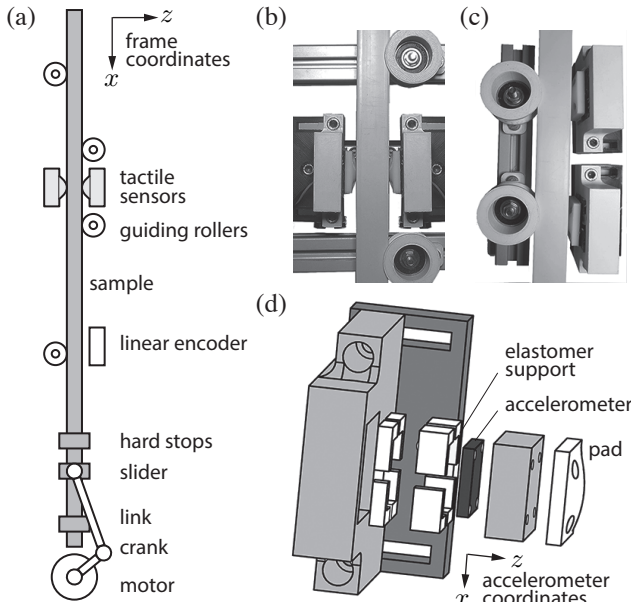


Fig. 2: Experimental setup. (A) The schematics of the mechanical and sensor components of the setup. (B) Gripping configuration. (C) One-sided foot configuration. (D) Details of the construction of the sensorized gripper pads.

## V. RESULTS

Figure 3 shows the ability of the algorithm to discriminate the absence of slip from the existence of slip. The heat map in Fig. 3A represents a two-dimensional histogram of the averaged value of the NCC measure for all trials under twenty-four conditions ( $3 \times 2 \times 4$ ) when the material was wood. The same data are shown in Fig. 3B in terms of mean, one standard deviation (dark gray), and two standard deviations (light gray). Fig. 3C represents the distribution of NCC values for slip and non-slip when speed is 0.2 m/s. The contact state was labeled ‘non-slip’ when the speed of the sample, as estimated from the encoder by the inverse time method [54], fell below a threshold of  $0.1 \text{ mm s}^{-1}$ . The contact state was labeled ‘slip’ above this threshold.

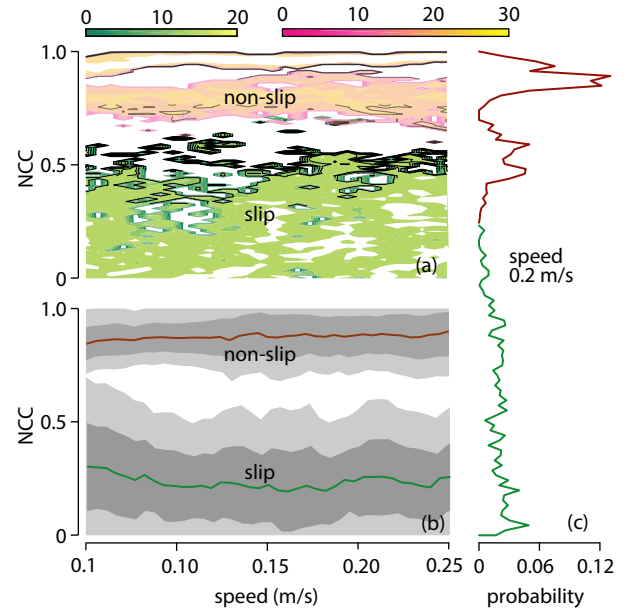


Fig. 3: Discrete probability density function (PDF) represented as a two-dimensional histogram of the NCC measure when the material was wood and the sensor orientation was zero. The color map represents values of the PDF in logarithmic scale. (A) PDFs represented as a two-dimensional histogram of the NCC measure. The color map represents values of the PDFs in a logarithmic scale. (B) The distribution of NCC values are shown in terms of mean and standard deviations. (C) PDFs of 0.2 m/s speed

The wooden sample is clearly a favorable case for the discrimination of non-slip and slip contact states. Figure 4 shows the Hellinger distance,  $H$ , computed for the sensor signals obtained between these two states when the optimal conditions were altered.

Figure 4A shows the evolution of  $H$  for different gripper orientations. It shows that the discrimination robustness, not the performance, was sensitive to the orientation and that the robustness was optimal when the acceleration was measured in the direction of slip, which makes sense intuitively. Figure 4B

TABLE I: Materials and interaction forces.

material	roughness [nm]	lower force [N]	higher force [N]
aluminum	121	15	25
plastic	372	20	35
wood	6381	6	12
glass	45	40	51

shows that the discrimination robustness of the system is greater for the gripping configuration than for the foot configuration. This result could be explained by the fact that the signal might have leaked between the two sensors in greater proportion for the foot configuration than for the gripper configuration, decreasing the distance between the signal acquired during the different contact states. Figure 4C reports what could be intuitively predicted, namely, that smoother surfaces decrease robustness. Finally, Fig. 4D shows that robustness is unaffected by the level of gripping force, which is also intuitively correct, since pressure is unlikely to modify the correlation of the frictional noise signals.

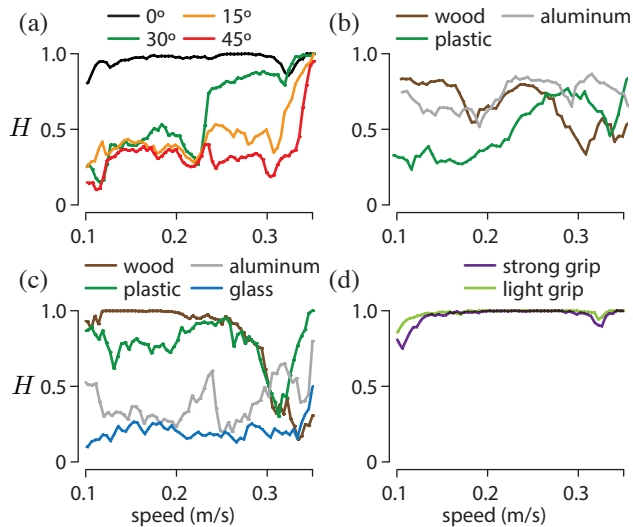


Fig. 4: Hellinger distance in different testing conditions. (A) Gripper orientation with respect to slip velocity. (B) One-sided foot configuration. (C) Material and roughness. (D) Grip force.

## VI. DISCUSSION AND CONCLUSION

The newly introduced non-slip detection algorithm by cross-correlation can compute a non-slip/slip decision within a few microseconds using an ordinary microcontroller. The decision delay is commensurate with the length of the buffer used to store past data. In the case of the present experiments, the length of this buffer was 500 samples, corresponding to 62.5 ms delay for a sampling rate of 8.0 kHz. Clearly, there are tradeoffs involved in the selection of the length of this buffer and the sampling rate: if the buffer is too short, the detection of decorrelation could be unreliable; if it is too long, the delay could become unacceptable. The sampling rate should be selected for a good representation of the signal. There is, however, a large range of values within which performance and robustness will be upheld. There is little tradeoff regarding the bandwidth of the sensors since frictional noise, except in pathological cases, always occurs over a large range of frequencies.

On this account, it should be noted that our non-slip detection algorithm would probably fail if the gripped object or if the stepped-upon ground violated the assumption of being a solid. If, for example, the held object is a fabric or a rope or if the ground is a granular material, then the pair of signals might decorrelate, even when no macroscopic slip takes place.

It should be recognized, however, that in these cases the very notion of absence of slip is elusive.

Besides its computational efficiency and absence of tuning, a prominent practical advantage of the algorithm is the low cost incurred for its implementation. Here, the sensors were consumer-grade, widely available mass-produced accelerometers. Many other types of sensors could be used for the purpose of responding to the vibrations of the pads in contact with objects or the ground. For example, low-cost monomorph disc piezoelectric units respond with high sensitivity to minute vibrations. Miniature microphones would also be applicable.

Another key advantage of this algorithm is its ability to be implemented as a retrofit on most existing robots, whether they have grippers, hands, feet, or even wheels. In the case of wheels, the implementation might not be straightforward because the sensors would have to be configured so that both are always in close vicinity of the contact with the ground. The signals would also have to be routed through the hubs. The algorithm could also be easily retrofitted in most motorized prosthetic hands and grippers with minimal effort. Lastly, not the least of these applications could be to human hands and feet since vibratory signals propagate the tissues of human extremities [55], [56]. Sensorized gloves and shoes could also be an interesting option.

It is tempting to draw parallels with human gripping. To date, research has focused on discovering tactile cues that can be used to detect slip. Westling and Johansson demonstrated that participants with anesthetized fingers would adjust their grip to the weight of objects but not to their frictional properties, thus demonstrating the existence of a physiological mechanism that responds to slip [57]. The authors later demonstrated that fast-adapting mechanoreceptors found in the glabrous skin of fingers responded before fully-developed slip takes place between fingers and counter-surfaces in suddenly loaded grips [6], [58]. A follow-up study confirmed through electromyography (EMG) that motor adjustment takes place about 130 ms after the start of an unexpected perturbation and, importantly, is time-locked with the onset of friction-induced vibrations [59]. The possibility exists that human gripping activity may depend on estimating the correlation—or the lack thereof—of sensor signals between or within fingers [7] on the grounds that estimating correlation is a fundamental computational process of neural systems [60].

## REFERENCES

- [1] Z. Stojiljković and J. Clot, "Integrated behavior of artificial skin," *IEEE Transactions on Biomedical Engineering*, vol. 4, pp. 396–399, 1977.
- [2] P. Dario and D. De Rossi, "Tactile sensors and the gripping challenge," *IEEE Spectrum*, vol. 22, no. 8, pp. 46–52, 1985.
- [3] H. R. Nicholls and M. H. Lee, "A survey of robot tactile sensing technology," *The International Journal of Robotics Research*, vol. 8, no. 3, pp. 3–30, 1989.
- [4] M. L. Hammock, A. Chortos, N. C.-K. Tee, J. B.-H. Tok, and Z. Bao, "25th anniversary article: The evolution of electronic skin (e-skin): a brief history, design considerations, and recent progress," *Advanced Materials*, vol. 25, no. 42, pp. 5997–6038, 2013.
- [5] R. Dahiya, N. Yogeswaran, F. Liu, L. Manjakkal, E. Burdet, V. Hayward, and H. Jörntell, "Large-area soft e-skin: The challenges beyond sensor designs," *Proceedings of the IEEE*, vol. 107, no. 10, pp. 2016–2033, 2019.

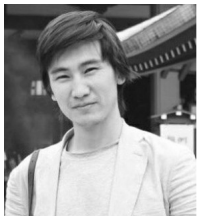
- [6] R. S. Johansson and G. Westling, "Signals in tactile afferents from the fingers eliciting adaptive motor responses during precision grip," *Experimental Brain Research*, vol. 66, no. 1, pp. 141–154, 1987.
- [7] B. Delhayé, E. Jarocka, A. Barrea, J.-L. Thonnard, B. Edin, and P. Lefèvre, "High-resolution imaging of skin deformation shows that afferents from human fingertips signal slip onset," *Elife*, vol. 10, p. e64679, 2021.
- [8] A. Bicchi, J. K. Salisbury, and P. Dario, "Augmentation of grasp robustness using intrinsic tactile sensing," in *Proc. of the IEEE International Conference on Robotics and Automation (ICRA)*, 1989, pp. 302–307.
- [9] T. Y. Hosoda, K. and M. Asada, "Internal representation of slip for a soft finger with vision and tactile sensors," in *Proc. of the IEEE/RSJ International Conference on Intelligent Robots and Systems (IROS)*, vol. 1, 2002, pp. 111–115.
- [10] A. Akay, "Acoustics of friction," *The Journal of the Acoustical Society of America*, vol. 111, no. 4, pp. 1525–1548, 2002.
- [11] M. J. Adams, S. A. Johnson, P. Lefèvre, V. Lévesque, V. Hayward, T. André, and J.-L. Thonnard, "Finger pad friction and its role in grip and touch," *Journal of the Royal Society Interface*, vol. 10, no. 80, p. 20120467, 2013.
- [12] D. Gueorguiev, S. Bochereau, A. Mouraux, V. Hayward, and J. L. Thonnard, "Touch uses frictional cues to discriminate flat materials," *Scientific Reports*, vol. 6, p. 25553, 2016.
- [13] W. H. Briscoe, S. Titmuss, F. Tiberge, R. K. Thomas, D. J. McGillivray, and J. Klein, "Boundary lubrication under water," *Nature*, vol. 444, no. 7116, pp. 191–194, 2006.
- [14] G. Tsoumis *et al.*, *Science and technology of wood: Structure, properties, utilization*. Van Nostrand Reinhold New York, 1991, vol. 115.
- [15] M. L. Oelze, O. W. D., and D. R. G., "Measurement of attenuation and speed of sound in soils," *Soil Science Society of America Journal*, vol. 66, no. 3, pp. 788–796, 2002.
- [16] H. Inoue, "Force feedback in precise assembly tasks," Massachusetts Institute of Technology, Artificial Intelligence Laboratory, Memo 308, 1974.
- [17] J. C. Baits, R. W. Todd, and J. M. Nightingale, "The feasibility of an adaptive control scheme for artificial prehension," in *Proc. of the Institution of Mechanical Engineers*, vol. 183. London, England: SAGE Publications, 1968, pp. 54–59.
- [18] N. D. Ring and D. B. Welbourn, "A self-adaptive gripping device: Its design and performance," in *Proc. of the Institution of Mechanical Engineers*, vol. 183. SAGE Publications, 1968, pp. 45–49.
- [19] A. V. Terekhov and V. Hayward, "Minimal adhesion surface area in tangentially loaded digital contacts," *Journal of Biomechanics*, vol. 44, no. 13, pp. 2508–2510, 2011.
- [20] D. Dornfeld and C. Handy, "Slip detection using acoustic emission signal analysis," in *Proc. of the IEEE International Conference on Robotics and Automation (ICRA)*, vol. 4, 1987, pp. 1868–1875.
- [21] R. Howe and M. Cutkosky, "Sensing skin acceleration for slip and texture perception," in *Proc. of the IEEE International Conference on Robotics and Automation (ICRA)*, vol. 1, 1989, pp. 145–150.
- [22] M. R. Tremblay and M. R. Cutkosky, "Estimating friction using incipient slip sensing during a manipulation task," in *Proc. of the IEEE International Conference on Robotics and Automation (ICRA)*, 1993, pp. 429–434.
- [23] P. J. Kyberd and P. H. Chappell, "Object-slip detection during manipulation using a derived force vector," *Mechatronics*, vol. 2, no. 1, pp. 1–13, 1992.
- [24] P. J. Kyberd, M. Evans, and S. te Winkel, "An intelligent anthropomorphic hand, with automatic grasp," *Robotica*, vol. 16, no. 5, pp. 531–536, 1998.
- [25] D. Göger, N. Gorges, and H. Worn, "Tactile sensing for an anthropomorphic robotic hand: Hardware and signal processing," in *Proc. of the IEEE International Conference on Robotics and Automation (ICRA)*, 2009, pp. 895–901.
- [26] S. Takenawa, "A magnetic type tactile sensor using a two-dimensional array of inductors," in *Proc. of the IEEE International Conference on Robotics and Automation (ICRA)*, 2009, pp. 3295–3300.
- [27] J. M. Romano, K. Hsiao, G. Niemeyer, S. Chitta, and K. J. Kuchenbecker, "Human-inspired robotic grasp control with tactile sensing," *IEEE Transactions on Robotics*, vol. 27, no. 6, 2011.
- [28] S. Teshigawara, T. Tsutsumi, S. Shimizu, Y. Suzuki, A. Ming, M. Ishikawa, and M. Shimajo, "Highly sensitive sensor for detection of initial slip and its application in a multi-fingered robot hand," in *Proc. of the IEEE International Conference on Robotics and Automation (ICRA)*, 2011, pp. 1097–1102.
- [29] B. Heyneman and M. R. Cutkosky, "Slip interface classification through tactile signal coherence," in *Proc. of the IEEE/RSJ International Conference on Intelligent Robots and Systems (IROS)*, 2013, pp. 801–808.
- [30] Z. Su, K. Hausman, Y. Chebotar, A. Molchanov, G. E. Loeb, G. S. Sukhatme, and S. Schaal, "Force estimation and slip detection/classification for grip control using a biomimetic tactile sensor," in *Proc. of the IEEE-RAS International Conference on Humanoid Robots (HUMANOIDS)*, 2015, pp. 297–303.
- [31] F. Veiga, H. van Hoof, J. Peters, and T. Hermans, "Stabilizing novel objects by learning to predict tactile slip," in *Proc. of the IEEE/RSJ International Conference on Intelligent Robots and Systems (IROS)*, . 2015, pp. 5065–5072.
- [32] V. A. Ho, T. Nagatani, A. Noda, and S. Hirai, "What can be inferred from a tactile arrayed sensor in autonomous in-hand manipulation?" in *Proc. of the IEEE International Conference on Automation Science and Engineering (CASE)*, 2012, pp. 461–468.
- [33] V. A. Ho and S. Hirai, "A novel model for assessing sliding mechanics and tactile sensation of human-like fingertips during slip action," *Robotics and Autonomous Systems*, vol. 63, pp. 253–267, 2015.
- [34] W. Yuan, R. Li, M. A. Srinivasan, and E. H. Adelson, "Measurement of shear and slip with a gelsight tactile sensor," in *Proc. of the IEEE International Conference on Robotics and Automation (ICRA)*, 2015, pp. 304–311.
- [35] M. K. Johnson, F. Cole, A. Raj, and E. H. Adelson, "Microgeometry capture using an elastomeric sensor," *ACM Transactions on Graphics*, vol. 30, no. 4, pp. 1–8, 2011.
- [36] M. Meier, F. Patzelt, R. Haschke, and H. J. Ritter, "Tactile convolutional networks for online slip and rotation detection," in *Proc. of the International Conference on Artificial Neural Networks*. Springer, 2016, pp. 12–19.
- [37] J. Roberge, S. Rispal, T. Wong, and V. Duchaine, "Unsupervised feature learning for classifying dynamic tactile events using sparse coding," in *Proc. of the IEEE International Conference on Robotics and Automation (ICRA)*, 2016, pp. 2675–2681.
- [38] J. W. James, N. Pestell, and N. F. Lepora, "Slip detection with a biomimetic tactile sensor," *IEEE Robotics and Automation Letters*, vol. 3, no. 4, pp. 3340–3346, 2018.
- [39] A. Rigi, F. B. Naeini, D. Makris, and Y. Zweiri, "A novel event-based incipient slip detection using dynamic active-pixel vision sensor (davis)," *Sensors*, vol. 18, no. 2, p. 333, 2018.
- [40] C. Melchiorri, "Slip detection and control using tactile and force sensors," *IEEE/ASME Transactions on Mechatronics*, vol. 5, no. 3, pp. 235–243, 2000.
- [41] N. Wettels, A. R. Parnandi, J.-H. Moon, G. E. Loeb, and G. Sukhatme, "Grip control using biomimetic tactile sensing systems," *IEEE/ASME Transactions on Mechatronics*, vol. 14, no. 6, pp. 718–723, 2009.
- [42] X. Song, H. Liu, K. Althoefer, T. Nanayakkara, and L. D. Seneviratne, "Efficient break-away friction ratio and slip prediction based on haptic surface exploration," *IEEE Transactions on Robotics*, vol. 30, no. 1, pp. 203–219, 2014.
- [43] C. Canudas De Wit, H. Olsson, K. J. Astrom, and P. Lischinsky, "A new model for control of systems with friction," *IEEE Transactions on automatic control*, vol. 40, no. 3, pp. 419–425, 1995.
- [44] H. Yussof, Z. Nur Ismarrubie, A. K. Makhtar, M. Ohka, and S. N. Basir, "Tactile slippage analysis in optical three-axis tactile sensor for robotic hand," *Applied Mechanics and Materials*, vol. 465, pp. 1375–1379, 2014.
- [45] R. Tomović and Z. Stojiljković, "Multifunctional terminal device with adaptive grasping force," *Automatica*, vol. 11, no. 6, pp. 567–570, 1975.
- [46] T. D'Alessio and R. Steindler, "Slip sensors for the control of the grasp in functional neuromuscular stimulation," *Medical Engineering & Physics*, vol. 17, no. 6, pp. 466–470, 1995.
- [47] F. Eghtedari, S. Hopkins, and D. Pham, "Model of a slip sensor," *Proc. of the Institution of Mechanical Engineers, Part B: Journal of Engineering Manufacture*, vol. 207, no. 1, pp. 55–64, 1993.
- [48] V. N. Dubey and R. M. Crowder, "A dynamic tactile sensor on photoelastic effect," *Sensors and Actuators A: Physical*, vol. 128, no. 2, pp. 217–224, 2006.
- [49] A. Gofuku, Y. Tanaka, and J. Tsubot, "Development of a flexible artificial hand system equipped with a slip sensor," *JSME International Journal Series C Mechanical Systems, Machine Elements and Manufacturing*, vol. 43, no. 2, pp. 378–386, 2000.
- [50] D. Accoto, R. Sahai, F. Damiani, D. Campolo, E. Guglielmelli, and P. Dario, "A slip sensor for biorobotic applications using a hot wire anemometry approach," *Sensors and Actuators A*, vol. 187, pp. 201–208, 2012.



- [51] Y. Kondratenko, O. Gerasin, and A. Topalov, "A simulation model for robot's slip displacement sensors," *International Journal of Computing*, vol. 15, no. 4, pp. 224–236, 2016.
- [52] B. G. Lindsay, "Efficiency versus robustness: the case for minimum hellinger distance and related methods," *The Annals of Statistics*, vol. 22, no. 2, pp. 1081–1114, 1994.
- [53] D. C. Dowson and B. V. Landau, "The Fréchet distance between multivariate normal distributions," *Journal of Multivariate Analysis*, vol. 12, no. 3, pp. 450–455, 1982.
- [54] B. Habibullah, H. Singh, K. Soo, and L. Ong, "A new digital speed transducer," *IEEE Transactions on Industrial Electronics and Control Instrumentation*, vol. IECI-25, no. 4, pp. 339–342, 1978.
- [55] Y. Shao, V. Hayward, and Y. Visell, "Spatial patterns of cutaneous vibration during whole-hand haptic interactions," *Proceedings of the National Academy of Sciences*, vol. 113, no. 15, pp. 4188–4193, 2016.
- [56] L. P. Kirsch, X. E. Job, M. Auvray, and V. Hayward, "Harnessing tactile waves to measure skin-to-skin interactions," *Behavior Research Methods*, pp. 1–9, 2020.
- [57] G. Westling and R. S. Johansson, "Factors influencing the force control during precision grip," *Experimental Brain Research*, vol. 53, no. 2, pp. 277–284, 1984.
- [58] —, "Responses in glabrous skin mechanoreceptors during precision grip in humans," *Experimental Brain Research*, vol. 66, pp. 128–140, 1987.
- [59] M. Wiertlewski, S. Endo, A. M. Wing, and V. Hayward, "Slip-induced vibration influences the grip reflex: A pilot study," in *Proc. of the World Haptics Conference (WHC)*, 2013, pp. 627–632.
- [60] B. B. Averbeck, P. E. Latham, and A. Pouget, "Neural correlations, population coding and computation," *Nature Reviews Neuroscience*, vol. 7, no. 5, pp. 358–366, 2006.



**Yerkebulan Massalim** is a research engineer in Actronika SAS, Paris, France. He received the B.Eng. in electrical engineering in 2017 and M.S. in robotics in 2020 from Nazarbayev University, Nur-Sultan, Kazakhstan. From 2017 to 2020, he worked as a hardware engineer on several embedded systems projects. His research interests are haptics, tactile sensing, embedded systems, and machine learning.

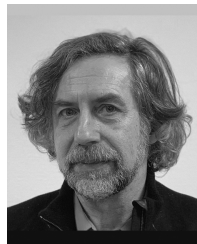


**Zhanat Kappassov** (M'16), received the Specialist degree in radioengineering from the Tomsk State of Control Systems and Radioelectronics (TUSUR), Tomsk, Russia. Afterward, he worked in the Industrial Technology Research Institute (ITRI), Taiwan. He received his Ph.D. in robotics from the Institute of Intelligent Systems and Robotics (ISIR), Sorbonne Université (formerly Université Pierre et Marie Curie), Paris, France, in 2017. He is currently an assistant professor of robotics at Nazarbayev University,

Nur-Sultan, Kazakhstan. His current research interests focus on tactile sensing for robot physical interaction and dexterous manipulation. He serves regularly as a reviewer for the IEEE Transactions on Robotics and IEEE conferences. His PhD thesis was nominated as the Best PhD Thesis 2017 by the GDR Robotique association in France.



**Huseyin Atakan Varol** (M'09-SM'16) received the B.S. degree in mechatronics engineering from Sabanci University, Istanbul, Turkey, in 2005, and the M.S. and Ph.D. degrees both in electrical engineering from Vanderbilt University, Nashville, TN, USA, in 2007 and 2009, respectively. From August 2009 to August 2011, he was first a postdoctoral research associate and then a research assistant professor with the Center for Intelligent Mechatronics, Department of Mechanical Engineering, Vanderbilt University, Nashville, TN, USA. In 2011, he joined the faculty of Nazarbayev University, Nur-Sultan, Kazakhstan, where he currently chairs the Department of Robotics and directs the Institute of Smart Systems and Artificial Intelligence (ISSAI). His research interests include soft robotics, machine learning, variable impedance actuation, tensegrity, and embedded systems. He has published over 70 technical papers on related topics in international journals and conferences. Dr. Varol was a finalist for the KUKA Innovation Award in 2014. He was also the recipient of the IEEE International Conference on Rehabilitation Robotics Best Paper Award in 2009 and IEEE Engineering in Medicine and Biology Society Outstanding Paper Award in 2013.



**Vincent Hayward** (M'84-SM'04-F'08) was a postdoctoral fellow, then a visiting assistant professor at Purdue University in 1982, and joined CNRS, France, as Chargé de Recherches in 1983. In 1989, he joined the Department of Electrical and Computer Engineering at McGill University as an assistant professor and became a full professor in 2006. He is now a professor at Sorbonne Université, Paris, France (formerly Université Pierre et Marie Curie). He has published in journals, conferences, collective books, co-founded spin-off companies, received best paper and research awards. He was on the editorial boards of the IEEE Transactions on Robotics, the ACM Transaction on Applied Perception, and the IEEE Transactions on Haptics. He was elected a member of the French Academy of Sciences in 2020.